Area-Perimeter Relation for Rain and Cloud Areas

S. Lovejoy

Science, New Series, Vol. 216, No. 4542 (Apr. 9, 1982), 185-187.

Stable URL:
http://links.jstor.org/sici?sici=0036-8075%2819820409%293%3A216%3A4542%3C185%3AARFRAC%3E2.0.CO%3B2-T

Science is currently published by American Association for the Advancement of Science.

mal part of the humerus. The digging stroke of proscalopids apparently required more retraction than that of talpids and more rotation than that of chrysochlorids. The broad glenoid fossa on the scapula, which would allow a considerable range of movement, also indicates that this was the case. The glenoid fossae of golden moles and true moles are narrow, confining the humerus mainly to retractional and rotational movements, respectively. The broad hand of proscalopids, although known only from fragmentary material, apparently resembled that of talpids more than that of chrysochlorids (*1, 9*).

The morphologic features of proscalopids indicate that their digging stroke combined an upward thrust of the head with a downward, posterior, and lateral movement of the hand. The stroke differed from that of chrysochlorids in that it allowed greater rotation of the humerus so that dirt could be moved laterally and because the hand could be used as a broad scoop. It differed from the stroke of talpids because the head was apparently thrust upward to displace dirt, and the humeri were retracted to apply counteracting downward forces at each of the hands. Such an arrangement would provide two directions of force so that the animal would be braced in the burrow as dirt was displaced in a third direction (*17*). The lateral orientation of thrust at the hands must have been less than that in talpids because the more laterally that this thrust is directed, the less the forelimbs would be capable of countering the upward movement of the head.

These differences between proscalopids and true moles suggest that the evolutionary history of the two groups is more distinct than has generally been recognized (*1, 3*). The fossorial specializations, rather than indicating affinities between the groups, indicate that proscalopids used a fundamentally different type of digging than true moles. Except for the broad hand, morphology associated with digging in proscalopids is confined to that group (that is, the humerus and vertebrae) or resembles that in chrysochlorids (that is, the skull, scapula, and clavicle). Similarities to chrysochlorids are probably due to evolution converging toward the use of the head in burrowing, because the zalambdodont dentition of golden moles is so different from the dilambdodont molars in proscalopids. Features not correlated with burrowing, such as the W-shaped ectoloph and complete zygomatic arch, may indicate that proscalopids are related to talpids at the superfamily level. The separate tibia and fibula of proscalopids suggest that these insectivores diverged from a form more primitive than any talpid, because in all talpids these bones are fused. It is unlikely that the morphology of the proscalopid humerus was derived from any known talpid because the pectoral process of even the most generalized true mole (*p* in Fig. 2C) has migrated toward the lesser tuberosity (*1*). In more advanced talpids these two structures meet to form the bicipital tunnel (Fig. 2A), a characteristic talpid feature that is absent in proscalopids. Furthermore, the earliest proscalopids (Chadronian) have specializations that are common to the group, and they appear on a different continent than the early talpids, which were confined to Europe and Asia until the middle Miocene (*3*). For these reasons, I concur with those who have suggested that the Proscalopidae represent a distinct family of insectivores (*1, 8*).

ANTHONY D. BARNOSKY
Department of Geological Sciences, University of Washington, Seattle 98195

References and Notes

1. C. A. Reed, W. D. Turnbull, *Fieldiana Geol.* **15**, 97 (1965).
2. J. H. Hutchison, *Nat. Hist. Mus. Los Angeles Cty. Contrib. Sci.* **235** (1972), pp. 1–16.
3. ———, *Bull. Mus. Nat. Hist. Univ. Oreg. 11* (1968), pp. 1–117.
4. P. R. Bjork, *J. Paleontol.* **49**, 808 (1975).
5. W. D. Matthew, *Science* **24**, 786 (1906).
6. R. Saban, *Bull. Mus. Natl. Hist. Nat. Ser. 2* **26**, 419 (1954).
7. G. G. Simpson, *Ann. Carnegie Mus.* **17**, 283 (1927).
8. K. M. Reed, *Bull. Mus. Comp. Zool. Harv. Univ.* **125**, 471 (1961).
9. See A. D. Barnosky, *J. Vertebr. Paleontol.* **1**, 285 (1981), for a description of the osteology and systematics of the new skeleton, which includes the skull and jaws, articulated vertebral column, articulated front leg except for the manus, manubrium, pelvis, femur, fibula, astragalus, and metatarsals. The fossil was found near White Sulphur Springs, Montana, by J. Rensberger of the University of Washington, and is housed at Burke Memorial Washington State Museum, University of Washington, No. 54708.
10. G. M. Puttick and J. U. M. Jarvis, *Zool. Afr.* **12**, 445 (1977).
11. V. C. Agrawal, *Mammalia* **31**, 300 (1967).
12. J. R. Slonaker, *J. Morphol.* **34**, 335 (1920).
13. C. A. Reed, *Am. Midl. Nat.* **45**, 513 (1951).
14. B. Campbell, *J. Mammal.* **19**, 234 (1938).
15. M. Hildebrand, *Analysis of Vertebrate Structure* (Wiley, New York, 1974).
16. D. W. Yalden, *J. Zool.* **149**, 55 (1966).
17. C. Reed and W. Turnbull, personal communication.
18. I thank C. Reed, W. Turnbull, and P. Bjork for helpful comments.

11 September 1981; revised 17 December 1981

Area-Perimeter Relation for Rain and Cloud Areas

Abstract. *Following Mandelbrot's theory of fractals, the area-perimeter relation is used to investigate the geometry of satellite- and radar-determined cloud and rain areas between 1 and 1.2 × 10^6 square kilometers. The data are well fit by a formula in which the perimeter is given approximately by the square root of the area raised to the power* D (P ~ $\sqrt{A^D}$), *where* D *is interpreted as the fractal dimension of the perimeter. It is concluded that rain and cloud perimeters are fractals—they have no characteristic horizontal length scale between 1 and 1000 kilometers.*

The diversity of cloud sizes and shapes is well known. No two clouds are alike, and while some can be measured in meters, others are as large as continents. Yet the "cloudlike" appearance of these shapes is seen even in the horizontal projections of clouds familiar to meteorologists in black-and-white satellite photographs. Similarly, rain areas as depicted by radar exhibit characteristic shapes that can help meteorologists to distinguish rainy regions from ground clutter (noise). Until recently, these simple geometric facts about clouds (and the associated rain areas) could not be incorporated directly into any theory, because of the lack of an appropriate geometric framework. However, since the publication of Mandelbrot's work on fractals (*1*), this situation has changed, and there are now simple methods for analyzing and modeling such shapes. In this report, we present the results of one such technique based on the area-perimeter relation, which indicates a remarkable constancy of the horizontal shapes of tropical clouds and rain areas over a range spanning six orders of magnitude in area. These findings lend support to the idea, first enunciated more than 50 years ago (*2*), that the outer limit of atmospheric turbulence may not be "attained within the atmosphere." This would mean that there is no special or preferred horizontal length scale for atmospheric processes, except scales of the order of the size of the earth. Shapes with structure at all scales, with no characteristic length, are known as fractals (*1*). Within the size range studied (1 km^2 to 1.2 × 10^6 km^2), cloud and rain areas are therefore fractals.

Mandelbrot (*1*) proposed using area-perimeter relations to investigate the structure of planar shapes. In the present study, the shapes considered are derived from digitized cloud and rain pictures on an approximately rectangular grid. These pictures define the projection of cloud and rain regions on the earth's

0036-8075/82/0409-0185$01.00/0

surface. The pictures are divided into either cloud–no cloud or rain–no rain regions, and individual clouds (or rain areas) are defined as a set of adjacent cloud (or rain) picture elements. Once the separate clouds (or rain areas) have been identified, the perimeter P and area A can be determined simply by counting the number of picture elements to determine the area and measuring the length of the cloud (or rain) boundary to determine the perimeter.

The A-P relation tells about the complexity, "wiggliness," or degree of contortion of the perimeter, since a fixed length of rounded, smooth perimeter can enclose a larger area than a complicated one can. This degree of complexity can be characterized by the dimension D of the perimeter, which appears in the formula $P \sim \sqrt{A}^D$. For smooth shapes such as circles and squares $P \sim \sqrt{A}$, and thus $D = 1$, the dimension of a line. As the perimeter becomes more and more contorted and tends to double back on itself, filling the plane, $P \sim A$, and D approaches the value 2. If the cloud or rain areas have structures with a well-defined length scale λ then we could consider the perimeter to be composed of large-scale structures (size $> \lambda$) with small-scale noise or perturbations (size $< \lambda$) superposed. Since the large- and small-scale structures would be different, they would have different A-P relations and thus different values of D. Consequently, if the A-P relation is characterized by different values of D for $A < \lambda^2$ and $A > \lambda^2$, then this would point to the existence of processes of size λ and lead to a meaningful distinction between a large and a small scale. Conversely, if the A-P relation is well described throughout by a relation of the form $P \sim \sqrt{A}^D$, this indicates the absence of characteristic length scales in the cloud (or rain) perimeters.

If $P \sim \sqrt{A}^D$ for rain and cloud areas, we may expect D to be an important parameter which characterizes the processes that produce clouds and rain. It is interesting to note that Kolmogorov's theory of isotropic, homogeneous turbulence in three dimensions (associated with the $-5/3$ power law energy spectrum) predicts $D = 5/3$ and $4/3$ for isotherms and isobars, respectively (*1*). This follows from the fact that for Kolmogorov turbulence, the standard deviation of the difference in temperature of two points separated by a distance r varies as $r^{1/3}$, while for pressure differences the analogous law is $r^{2/3}$ (*3*).

The analysis of the A-P relation is thus complementary to the harmonic analysis of stochastic functions (analogous to Fourier analysis) and has the advantage that it is applicable in some cases where harmonic analysis is not. In particular, there is evidence (*4*) that rain fields fluctuate so erratically that they might not be amenable to harmonic analysis. In any case, the A-P analysis is quite simple and was automatically performed on the digitized radar and satellite data available.

Figure 1 shows the A-P relation for radar pictures of tropical rain areas at a resolution of 1 by 1 km and for infrared pictures of Indian Ocean clouds, sampled on a grid of 4.8 by 4.8 km (*5*), from the geostationary operational environment satellite (GOES). Taken separately, the radar and satellite data fall on parallel straight lines. When the satellite perimeters are multiplied by a correction factor (explained below), these two lines coincide as shown and yield a least squares estimate of $D \sim 1.35$ with correlation coefficient .994. A correction factor is required because the radar data have a different spatial resolution from the satellite data and thus are more sensitive to the detailed structure of a perimeter. For a given area, the radar will therefore always measure a longer perimeter than the satellite. It may be shown (*1*) that if the perimeter is a fractal of dimension D, the length of a perimeter measured at resolution L_1 is greater than the length of one measured at L_2 by the factor $(L_1/L_2)^{1-D}$. The satellite perimeters were therefore multiplied by the factor $(1/4.8)^{-0.35} = 1.73$ to make them compatible with the radar data.

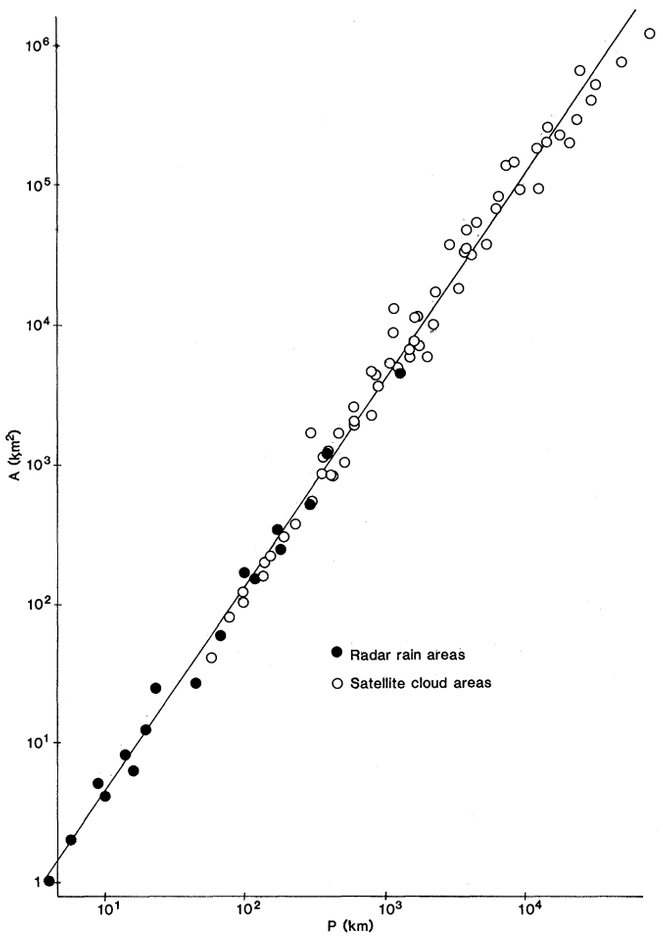

Fig. 1. Area plotted against perimeter of rain and cloud areas determined from radar and satellite data.

Physically, the radar senses reflected microwave radiation, primarily from the large raindrops. The rain areas were defined as those regions for which the rain rate exceeded 0.2 mm/hour (which corresponds to a light drizzle). Because of the curvature of the earth, reliable radar coverage is limited to an area $\lesssim$ 40,000 km^2. In order to extend the range of scales amenable to study, it is necessary to supplement the radar data with other data at larger scales. Although rainfall data suitable for this purpose are not available, cloud data from GOES provide coverage of a large fraction of the earth's surface, with a resolution of $\sim$ 6.4 km in the infrared. The higher resolution visible channel was not used because of the problem of varying sun and satellite angles of this reflected light. The GOES infrared sensor responds pri-

marily to the blackbody radiation emitted by the clouds and surface, which is isotropic. At these wavelengths, clouds more than about 300 m thick emit as blackbodies (*6*), and therefore the infrared channel yields an estimate of the cloud-top temperature. If the vertical temperature profile is known, the height of the cloud top can be determined.

In Fig. 1 the threshold defining cloud areas is somewhat arbitrarily set at −10°C for the cloud-top temperature. If the threshold is raised too much, we risk including parts of the ocean in our cloud areas. If it is lowered too much, we obtain very few regions of appreciable extent. The choice of −10°C is a compromise between these extremes. Some experimentation with different thresholds (−15° and −5°C) yielded similar results. Changing the threshold decreases or increases the size of the clouds for colder or warmer thresholds, respectively. However, the perimeters change in such a way that the points remain on the line shown in Fig. 1.

Physically, the rain and cloud fields are closely related in the tropics, since both occur in regions of convective updraft, which causes the moist warm surface air to rise, cool by adiabatic expansion, and form clouds and rain in the resulting condensation processes. Because of the relatively short time scale of these processes, much of these clouds, even at −20° or −30°C, is supercooled water rather than ice. The cloud area delineated by the −10°C threshold thus contains regions of both cumulus and cirrus clouds (composed mainly of supercooled droplets and ice particles, respectively).

For convenience, GOES pictures of the Indian Ocean region sampled at resolutions of 4.8 and 19.2 km were used. To avoid effects of varying picture element size, primarily due to the earth's curvature, only data in the relatively undistorted region between 20°N and 20°S and within ± 30° of longitude of the subsatellite point were used. Because effects due to the earth's curvature are similar for both area and perimeter, the A/P ratio is affected only to second order. Therefore image distortion should not yield a systematic effect in Fig. 1, even for the largest cloud examined, which extended over 3000 km from Africa to south of India (with an area of $\sim 1.2 \times 10^6$ km^2).

The most striking aspect of Fig. 1 is the absence of any apparent bend or kink over the range of more than six orders of magnitude in area. This is important because the evidence to date, based largely on Fourier spectra of wind variations, has been inconclusive about the existence of length scales, particularly in the range 1 to 1000 km. Theoretically, such a length scale might arise because of the gradual transition from a three-dimensional turbulent regime at small scales to a two-dimensional regime at a scale of hundreds of kilometers, where the atmosphere would appear thin (the scale height of the atmosphere is ~ 10 km). Indeed, early investigations pointed to the existence of a "mesoscale gap" in wind spectra [for instance (*7*)]. However, later research showed this situation to be the exception rather than the rule (*8*) and indicated no break in the spectrum for distances up to at least 1000 km. Experiments with high-altitude balloons also failed to show evidence of a length scale in the range 100 to 1000 km (*9*), and clear air Doppler radar wind measurements showed no length scales in the range 4 to 400 km (*10*). Recently, Doppler wind spectra in rainy regions failed to show any evidence of length scales in the range 1.6 to 25 km (*11*).

Although higher resolution radar or satellite data are needed to extend Fig. 1 in the direction of smaller A, other experiments, such as aircraft measurements of wind spectra (*12*), found no evidence of length scales down to 10 m. Indeed, as Richardson's (*13*) famous atmospheric diffusion experiment suggested, the range of scaleless behavior may continue down to distances of centimeters, where viscosity becomes important. If Richardson was right, then a fractal model of the atmosphere may be appropriate over a large fraction of the range of meteorologically significant distances.

Finally, it is interesting to speculate on the empirical value of D obtained from Fig. 1. The value 1.35 is so close to the value 4/3 (that of turbulent isobars) that some fairly straightforward connection may exist. An understanding of the physical origins of this value could therefore be important.

S. LOVEJOY

Centre de Recherches Atmosphériques de Magny les Hameaux, 78470 Saint Remy les Chevreuse, France

References and Notes

1. B. Mandelbrot, *Fractals* (Freeman, San Francisco, 1977).
2. L. F. Richardson, *Proc. R. Soc. London Ser. A* **110**, 709 (1926).
3. G. K. Batchelor, *The Theory of Homogeneous Turbulence* (Cambridge Univ. Press, New York, 1953).
4. S. Lovejoy, *Preprint Volume, 20th Conference on Radar Meteorology* (American Meteorological Society, Boston, 1981), p. 476.
5. The intrinsic resolution of the satellite sensor is 6.4 km, but the data available on magnetic tape were sampled at 4.8 km to be compatible with the data from the higher resolution visible sensor.
6. F. Mosher, thesis, University of Wisconsin, Madison (1979).
7. J. Van der Hoven, *J. Meteorol.* **14**, 160 (1957).
8. N. K. Vinnichenko, *Tellus* **22**, 158 (1970).
9. P. Morel and M. Larcheveque, *J. Appl. Meteorol.* **31**, 2189 (1974).
10. K. S. Gage, *J. Atmos. Sci.* **36**, 1950 (1979).
11. M. Gilet, S. Nicoloff, V. Klaus, C. Gaillard, *Preprint Volume, 19th Conference on Radar Meteorology* (American Meteorological Society, Boston, 1980), p. 30.
12. J. I. MacPherson and G. A. Isaac, *J. Appl. Meteorol.* **16**, 81 (1977).
13. L. F. Richardson, *Beitr. Phys. Freien Atmos.* **15**, 24 (1929).
14. I thank B. Mandelbrot, G. L. Austin, J. C. André, D. Schertzer, M. Gilet, and U. Phadke for helpful discussions and comments.

4 August 1981; revised 30 December 1981

Maceral, Total Organic Carbon, and Palynological Analyses of Ross Ice Shelf Project Site J9 Cores

Abstract. *Analyses of macerals and total organic carbon indicate that the low organic content of core sediments from Ross Ice Shelf Project site J9 has been selectively reduced further, probably by postdepositional submarine oxidation. Palynological analysis revealed a reworked Paleogene dinocyst flora of low diversity (the transantarctic flora). This constitutes the most southerly dinocyst flora reported thus far. The antarctic distribution of the transantarctic flora supports the existence of a transantarctic strait during the Paleogene. The J9 sporomorph assemblage also is reworked and Paleogene in age.*

Gravity cores recovered by the Ross Ice Shelf Project from site J9 (82°22′S, 168°38′W) have provided the first bottom sediments from beneath the southern Ross Ice Shelf for scientific research (*1*). Maceral and total organic carbon (TOC) analyses were conducted on core samples to document the types and distribution of macerals present, to determine the TOC profiles, and to study the effects of reported submarine oxidation on the maceral and TOC contents. A preliminary palynological investigation also has been conducted on a low-diversity palynoflora observed during maceral analysis (*2*).

Previous sedimentological investigations have demonstrated the presence of two lithologic units in each core (*1*). The lighter colored upper unit (unit 2) is an

0036-8075/82/0409-0187$01.00/0